The BAF (BRG1/BRM-Associated Factor) Chromatin-Remodeling Complex Exhibits Ethanol Sensitivity in Fetal Neural Progenitor Cells and Regulates Transcription at the Mir-9-2 Encoding Gene Locus

Sasha G. Burrowes[#], **Nihal A. Salem**[#], **Alexander M. Tseng**[#], **Sridevi Balaraman**, **Marisa R. Pinson**, **Cadianna Garcia**, and **Rajesh C. Miranda**[*]

Dept. Neuroscience and Experimental Therapeutics & Women's Health in Neuroscience Program, College of Medicine, Texas A&M Health Science Center

Abstract

Fetal alcohol spectrum disorders are a leading cause of intellectual disability worldwide. Previous studies have shown that developmental ethanol exposure results in loss of microRNAs (miRNAs) including miR-9, and loss of these miRNAs, in turn, mediates some of ethanol's teratogenic effects in the developing brain. We previously found that ethanol increased methylation at the miR-9-2 encoding gene locus in mouse fetal neural stem cells (NSC), advancing a mechanism for epigenetic silencing of this locus and consequently, miR-9 loss in NSCs. Therefore, we assessed the role of the BAF (BRG1/BRM-Associated Factor) complex, which disassembles nucleosomes to facilitate access to chromatin, as an epigenetic mediator of ethanol's effects on miR-9. Chromatin immunoprecipitation and DNAse-I hypersensitivity analyses showed that the BAF-complex was associated with both transcriptionally accessible and heterochromatic regions of the miR-9-2 locus, and that disintegration of the BAF-complex by combined knockdown of BAF170 and BAF155 resulted in a significant decrease in miR-9. We hypothesized that ethanol exposure would result in loss of BAF-complex function at the miR-9-2 locus. However, ethanol exposure significantly increased mRNA transcripts for maturation-associated BAF complex members, BAF170, SS18, ARID2, BAF60a, BRM/BAF190b and BAF53b. Ethanol also significantly increased BAF-complex binding within an intron containing a CpG island and in the terminal exon encoding precursor (pre)-miR-9-2. These data suggest that the BAF complex may adaptively respond to ethanol exposure to protect against a complete loss of miR-9-2 in fetal NSCs. Chromatin remodeling factors may adapt to the presence of a teratogen, to maintain transcription of critical miRNA regulatory pathways.

[*]Corresponding author: Contact Address: Texas A&M Health Science Ctr., College of Medicine, Dept. Neuroscience & Experimental Therapeutics, Medical Research and Education Bldg., 8447 State Highway 47, Bryan, TX 77807-3260, phone: 979-436-0332, fax: 979-436-0086, miranda@medicine.tamhsc.edu.

[#]Authors contributed equally to the reported experiments

Introduction

Fetal alcohol spectrum disorders (FASDs), are a leading cause of intellectual disability in the US and worldwide, with an estimated global prevalence of ~2.3% (Roozen et al., 2016). Despite long-term evidence that alcohol is teratogenic (Jones et al., 1973; Lemoine et al., 1968), FASDs remain difficult to prevent in the US, due in part, to the combined prevalence of unplanned pregnancies (Finer and Zolna, 2016) and patterns of heavy alcohol consumption, particularly binge-type consumption, among women of child-bearing age (Tan et al., 2015). Such socio-cultural influences increase the risk for inadvertent prenatal alcohol exposure, particularly during the first and second trimesters, when fetal neural stem cells (NSCs) produce most of the neurons of the adult brain (Bystron et al., 2008). The worldwide persistence of FASD is a challenging public health problem and emphasizes the need to identify aspects of alcohol teratogenicity that can be mitigated by early intervention.

In rodent models, alcohol exposure during the first trimester-equivalent period was shown to reduce neurogenesis (Miller, 1989) and decrease the thickness of the NSC-enriched fetal cortical ventricular neuroepithelium (Sudheendran et al., 2013), resulting in persistent brain growth deficits (Maier et al., 1999). However, surprisingly, research in *ex vivo* rodent models of fetal NSCs showed that ethanol exposure did not result in cell death (Prock and Miranda, 2007; Santillano et al., 2005), but rather NSC loss, due to increased proliferation associated with premature and aberrant maturation (Camarillo and Miranda, 2008; Miller and Nowakowski, 1991; Santillano et al., 2005; Tingling et al., 2013). We further determined that many effects of ethanol on fetal NSCs and early embryogenesis were mediated by repression of a class of non-protein-coding regulatory microRNAs (miRNAs, (Pappalardo-Carter et al., 2013; Sathyan et al., 2007; Tsai et al., 2014)). The miRNA, miR-9 in particular, is an important regulator of brain segmentation (Leucht et al., 2008) and neuronal maturation (Shibata et al., 2008; Shibata et al., 2011), and is suppressed by ethanol during development in both mouse and zebrafish neural tissues (Pappalardo-Carter et al., 2013; Sathyan et al., 2007; Tal et al., 2012), but induced in the adult mouse brain (Pietrzykowski et al., 2008). Moreover, loss of miR-9 in a zebrafish embryo recapitulated craniofacial (Pappalardo-Carter et al., 2013) and behavioral (Tal et al., 2012) defects associated with prenatal ethanol exposure. However, the mechanisms whereby prenatal alcohol exposure (PAE) alters miRNAs in neural stem cells are unclear.

PAE is known to broadly interfere with epigenetic programming in fetal NSCs (Liu et al., 2009; Veazey et al., 2013; Veazey et al., 2015; Zhou et al., 2011). Moreover, epigenetic alterations persist, and can be assayed in more differentiated cells and tissues obtained from FASD children (Laufer et al., 2015; Masemola et al., 2015; Portales-Casamar et al., 2016). In an initial study, we found evidence that ethanol exposure resulted in increased methylation in fetal mouse neuroepithelial cells, specifically at the miR-9-2 gene locus, and not the miR-9-1 and miR-9-3 gene loci (Pappalardo-Carter et al., 2013). These data

suggested that epigenetic silencing of miRNA genes may mediate ethanol effects. In this study, we therefore assessed the effects of ethanol on methylation across the murine chromosome-13 locus encoding the primary miRNA transcript, pri-miR-9-2.

Mechanisms that facilitate chromatin access through nucleosome disassembly are a potentially important but uninvestigated epigenetic mediator of PAE. The SWI/SNF (Switch/ Sucrose Non-Fermentable)/BAF (BRG1/BRM-Associated Factor) heteromeric chromatin remodeling complex, a combinatorial assembly of ~10–15 different proteins assembled from 29 different gene products, causes ATP-dependent dis-assembly of nucleosomes by dissociating histones from DNA, to facilitate chromatin-remodeling and transcriptional activation (reviewed in (Kadoch et al., 2016)). The BAF complex controls neural stem cell maturation (Lessard et al., 2007; Yoo et al., 2009), and while component members change through the process of neural differentiation to promote neuron-specific chromatin remodeling (Vogel-Ciernia and Wood, 2014), the core catalytic subunits of the BAF complex, BRG1 (SMARCA4/BAF190A) and BRM (SMARCA2/BAF190B) remain constant. In humans, BRG1, BRM and other BAF-complex mutations result in significant intellectual disability, craniofacial abnormalities and growth deficits (Kosho and Okamoto, 2014; Van Houdt et al., 2012), and mice heterozygous for a BRG1 null mutation exhibit exencephaly (Bultman et al., 2000), all of which are phenotypes that have been associated with FASD.

A previous study showed that ethanol increased methylation of SMARCA2 (Zhou et al., 2011) in NSCs, suggesting that the BAF complex itself is an epigenetic target of ethanol. Moreover, in adult invertebrate and rodent vertebrate models, the BAF complex (Mathies et al., 2015) and miR-9 (Pietrzykowski et al., 2008), respectively, have both been shown to mediate acute tolerance to alcohol, suggesting a mechanistic linkage between miR-9 and the BAF complex. Therefore, in the current study, we investigated the effect of ethanol on the BAF complex in fetal NSCs, and the impact of the BAF complex on the gene locus encoding one of the miR-9 genes, miR-9-2, which had been previously identified (Pappalardo-Carter et al., 2013) as an epigenetic target of ethanol.

Methods

Ex-vivo fetal mouse neurosphere cultures

Neuroepithelial cells from the dorsal telencephalic vesicle, corresponding regional precursor of the murine iso-cortex were microdissected from gestational day (GD) 12.5 mouse fetuses as previously published (Prock and Miranda, 2007; Santillano et al., 2005; Sathyan et al., 2007; Tsai et al., 2014). All procedures were as approved by the Texas A&M University Committee on Animal Care (IACUC). Cells were maintained as non-adherent cultures in defined culture medium, resulting in the formation of neurospheres, an *ex vivo* cell culture model system of the fetal neural stem cell niche (Miranda et al., 2008). For all experiments, total cell counts were determined using a hemocytometer. Dispersed neuroepithelial precursors were established in culture at an initial density of 10^6 cells in T-25 flasks containing serum-free mitogenic media. Cells were allowed to proliferate as neurospheres until cultures achieved a density of 2×10^6 cells per T-25 flask, then randomly assigned to control (0 mg/dL) or ethanol treatment groups (120mg/dL (26mM) and 320 mg/dL

(70mM)), capped tightly with phenolic caps, and sealed with parafilm to limit the loss of ethanol. Ethanol concentrations in culture media were monitored by gas chromatography as previously published (Prock and Miranda, 2007; Santillano et al., 2005). Cultures were treated with ethanol for 5 days to mimic exposure through the period of neurogenesis and medium was changed every 2 days.

Differentiation paradigm—We previously showed that neurospheres cultured on a laminin substrate, and maintained in the absence of bFGF, became adherent and underwent terminal differentiation into migratory, bi-polar cells that expressed markers of neuronal identity (Camarillo and Miranda, 2008). Neurosphere cultures were suspended in media without bFGF, but supplemented with BDNF (25 ng/ml), and plated on laminin-coated (1.2 mg/ml, Thermo Fisher Scientific, Waltham, MA) 12-well plates. Culture medium was replaced every day. Photomicrographs were obtained every 24 hours over a 3-day period.

Quantitative Reverse Transcription Polymerase Chain Reaction (qRT-PCR)

qRT-PCR was used to examine mRNA levels of the BAF complex subunits. Three intron-spanning PCR primer sequences pairs were obtained for each gene of interest using NCBI Primer-BLAST program (Ye et al., 2012). Primer sequences were assessed for dimerization potential using IDT Oligo Analyzer 3.1 (Integrated DNA Technologies, Coralville, IA) and gene specificity and localization assessed via UCSC genome browser (Kent et al., 2002) *in-silico* PCR tool. Primers were then tested in duplicates using 250ng of cDNA harvested from GD12.5 murine neural stem cells, and thermal stability curves were assessed for evidence of a single amplicon. Selected amplicons were verified by sequencing (Texas A&M University Gene Technologies Lab) and compared to GenBank reference sequences for the gene of interest. Primer sequences are indicated in Table 1. RNA from neurospheres was isolated using Nucleospin columns (Macherey-Nagel, Bethlehem, PA) and cDNA were synthesized using qScript™ cDNA SuperMix (Qiagen).

Immunoprecipitation and Western Blot Analysis

Protein was extracted using 1X RIPA lysis buffer (EMD Millipore) supplemented with Halt protease inhibitor cocktail (Thermo Fisher Scientific). Protein concentration was determined using Pierce BCA protein assay kit (Thermo Fisher Scientific) and 25 μg of protein was loaded onto 3–8% Tris acetate gel (Invitrogen), run at 150 volts for 60 min, and transferred to a PVDF membrane using the iBlot transfer system (Invitrogen/ Thermo Fisher Scientific). The membrane was then blocked with 5% nonfat dry milk and 2.5% goat serum in Tris-buffered saline containing Tween-20 (TTBS) for 1 h and incubated overnight with anti-BRG1 antibody (Bethyl Laboratories, Montgomery, TX, A300–813A, dilution 1:1,000). The blot was then washed and incubated with an HRP-conjugated goat anti-rabbit IgG (Invitrogen) at dilution 1:1000 for 1 h then developed using PerkinElmer Western Lightning Plus Chemi ECL (PerkinElmer, Waltham, MA) and visualized using a CCD camera (Fluorchem Q, Alpha Innotech, San Leandro, CA). For the immuno-precipitation assays, 8 μl of anti-BRG1 or goat anti-rabbit IgG was added to fixed neurosphere lysates and incubated overnight followed by 1 h incubation with Dynabeads conjugated with protein-G (Thermo Fisher Scientific) for magnetic separation. Following washes, 20 μl of the bead/antibody/lysate solution were boiled with Laemmli buffer at 90°C for 10 minutes, loaded

onto a Tris-acetate gel, subjected to electrophoresis, transferred to a PVDF membrane and detected as detailed above. HRP-conjugated Protein-A (Thermo Fisher Scientific, dilution 1:20000) was used to detect the primary antibodies instead of goat anti-rabbit to avoid detection of heavy and light chains of the antibody used for immuno-precipitation.

Chromatin Immunoprecipitation (ChIP)

Control and ethanol-treated neurospheres were fixed in 1% paraformaldehyde and nuclear lysates were obtained using NE-PER Nuclear and Cytoplasmic Extraction Reagents supplemented with Halt protease inhibitor cocktail (Thermo Fisher Scientific). Samples were then sonicated in an iced water bath sonicator for alternating on/off in 30 sec intervals for ten minutes. Appropriate sonication time was validated by size-fractionation on an agarose gel to verify appropriate fragmentation. The sonicated nuclear lysate was then treated with either anti-BRG1 antibody or goat anti-rabbit IgG (Thermo Fisher Scientific) and incubated overnight. Protein G Dynabeads (Thermo Fisher Scientific) were blocked with salmon sperm DNA (0.3 mg/ml of beads, Invitrogen/ Thermo Fisher Scientific) and then added to the samples and incubated for one hour. Dynabeads were separated using a DynaMag magnet (Thermo Fisher Scientific) then washed twice in 0.05% Tween-20 in 1X PBS, and once 0.02% Tween-20 in 1X PBS. Beads were re-suspended in 0.02%Tween-20 in 1X PBS with 2 µl RNase A (0.5 mg/ml), and samples incubated at 65°C for 4 h to reverse the crosslinking. 2 µl proteinase K (20 mg/ml) was then added and the samples were incubated at 45°C for 1 h. DNA was purified using chloroform/isoamyl alcohol (EMD Millipore, Billerica, MA) isolation followed by ethanol precipitation.

siRNA Knockdown

Neurospheres were suspended into single cells suspension and plated in 24-well cell culture plates. Accell siRNA reagents (GE Dharmacon, Lafayette, CO) were used to knockdown BAF150 and BAF170. Accell Mouse Smarcc1 (E-044249) siRNA and Accell Mouse Smarcc2 (E-042842) siRNA – SMARTpool were delivered together to culture wells at a final concentration of 1µM each. Accell Non-targeting Pool (siRNA control, D-001910-10) was delivered to control wells at 2µM final concentration and Accell Cyclophilin B Pool (D-001920-20) was used to assess the transfection efficiency. After 72 hours of transfection, RNA was isolated by the Qiagen miRNeasy micro kit (Qiagen). The Quanta qScript cDNA Supermix (Quanta Biosciences, Beverly, MA) was used for first strand cDNA synthesis. Knock down of BAF150 and BAF170 was confirmed using qRT-PCR. After knockdown, miR-9 expression levels were analyzed using the Exiqon miRCURY LNA Universal RT microRNA cDNA synthesis kit (Exiqon A/S, Vedbaek Denmark) was used to synthesize cDNA qRT-PCR, which was subsequently performed using a commercial miR-9 primer set (Exiqon, #202240) with the small nuclear RNA, U6 (Exiqon, #203907), as a loading control

Identifying presumptive pri-miR-9-2 regulatory regions in the mouse genome

The ENCODE project analysis hub track in the UCSC genome browser was used to locate identified transcription regulatory factor binding sites for POU5F1/Oct4, c-myc and REST within the human pri-miR-9-2 gene locus (LINC00461, GRCh37/hg19 genome assembly, chr5:87,960,263-87,969,146), and syntenic mouse locus encoding ENSMUST00000131907/ C130071C03Rik, the mouse pri-mir-9-2 region (mouse assembly NCBI37/mm9,

chr13:83,867,711-83,875,274, UCSC genome browser, genome.ucsc.edu, (Kent et al., 2002)). Homologous regions in human and mouse pri-miR-9-2 encoding transcription factor binding domains (c-myc, Oct4/Pou5f1 and REST), pre-miR-9-2 coding regions, as well as CpG islands were identified and primers were designed using NCBI primer blast tool (Table 2).

Assessing DNAse I hypersensitive sites in pri-miR-9-2

Nuclei were obtained from mouse neurosphere cultures using the NE-PER Nuclear and Cytoplasmic Extraction Reagents (Thermo Fisher Scientific). Briefly, cells were concentrated into a pellet by centrifugation, and incubated with CER I buffer for ten minutes followed by CER II for one minute to lyse cell membranes. Then the samples were centrifuged and the cytoplasmic fraction was transferred into a new tube. The nuclear pellet was washed once with 1X PBS. As described in (Follows et al., 2007), nuclear pellets were treated with either 0, 20, 60 or 120U of DNAse I (Ambion/Thermo Fisher Scientific) for one hour on ice. The nuclei were then lysed open using NER buffer, and fragmented DNA was purified using isoamyl alcohol-chloroform. Digestion into 200–500bp fragments was confirmed by size fractionation on an agarose DNA gel, and fragmented DNA was then blunt ended using T4 polymerase, followed by ligation to a double stranded linker DNA. A biotinylated probe against the linker was used to create a complementary DNA strand for the ligated fragments and captured using streptavidin-coated Dynabeads (Dynabeads® M-270 Streptavidin, Thermo Fisher Scientific). The captured fragments represent DNAse I hypersensitive sites within the genome. DNA was eluted from the beads by heating at 95 °C for ten minutes. Eluted fragments from the 0U DNAse group represent the baseline fragmentation resulting from the technical shearing of DNA during pipetting and purification steps. Quantitative qPCR analysis was performed on the eluted DNA using the primers specific for the miR-9-2 gene including regions encoding the primary (pri-miR-9-2) and precursor (pre-miR-9-2) transcripts.

Statistical analysis

Cycle thresholds (CTs) obtained from qRT-PCR and qPCR analyses were analyzed statistically as change in CTs (ΔCTs) and graphically represented as fold-change ($2^{-\Delta CT}$). We used standard multivariate (MANOVA, Pillai's trace statistic) and univariate (ANOVA) parametric analysis models, and t-tests where appropriate. For post-hoc examination, the Fisher's least significant difference (LSD) test was chosen for pairwise comparisons (SPSS v24, IBM, Armonk, NY). Comparisons were assessed as statistically significant at $p<0.05$.

Results

Ethanol induces expression of components of the heteromeric BAF complex

Neurosphere cultures were exposed to control medium or to ethanol at 120mg/dl (26mM) and 320mg/dl (70mM) for 5 days to mimic moderate to heavy exposure during the *in vivo* period of neurogenesis in the mouse as previously published (Balaraman et al., 2012; Tsai et al., 2014). RNA extracted from ethanol exposed neural stem cells was used to analyze transcript levels of BAF complex subunits by qRT-PCR. Multivariate analysis (of ΔCTs) showed that there was an overall effect of ethanol exposure on BAF-complex mRNAs

(Pillai's Trace Statistic, $F_{(30,4)}$=67.579, p<0.001). Post-hoc univariate ANOVA (p<0.05) indicated that ethanol exposure specifically, and contrary to our hypothesis, resulted in dose-related increases in BAF170 ($F_{(2,15)}$=15.01,p<0.001), SS18 ($F_{(2,15)}$=28.48, p<0.001), ARID2 ($F_{(2,15)}$=6.59, p= 0.009), BAF60a ($F_{(2,15)}$=3.73, p= 0.049) and Smarca2/BRM/BAF190b ($F_{(2,15)}$=4.25, p= 0.035, significantly different at 120mg/dl) and BAF53b ($F_{(2,15)}$=4.84, p=0.024, significantly different the 320mg/dl), (Figure 1a). In contrast, mRNA levels for Cor1/SYCP3, BAF57, BAF53A, PHF10, DPF3, BAF155, BRG1, CREST and ACBT in NSCs were unaffected by ethanol exposure (all p's>0.05). These data indicate that ethanol exposure results in increased expression of both core and maturation-associated components of the BAF complex (Figure 1b, adapted from (Ho and Crabtree, 2010)).

Ethanol-sensitive BAF-complex components are also transiently induced during neural differentiation

Neurosphere cultures were differentiated over a three-day time course using a mitogen-withdrawal, BDNF-exposure paradigm, and mRNA levels of ethanol-affected subunits were measured. Multivariate analysis showed a significant overall effect of differentiation state on BAF complex transcripts ($F_{(21,36)}$=2.96, p<0.002). Post-hoc ANOVAs showed that Smarca2/Baf19b ($F_{(3,16)}$=9.56, p<0.001), ARID2 ($F_{(3,16)}$=6.39, p<0.005), Smarcc2/BAF170 ($F_{(3,16)}$=4.72, p<0.015), SS18 ($F_{(3,16)}$=5.57, p<0.017) and Actl6b/BAF53B ($F_{(3,16)}$=42.93, p<0.001) were all significantly altered during NSC differentiation (Figure 2). However, the expression of Smarcd1/BAF60a and BAF155 mRNA transcripts were not significantly changed.

Chromatin immuno-precipitation (ChIP) indicates that BRG1-containing complexes associate with both DNAse-hypersensitive and insensitive sites on the pri-miR-9-2 gene locus

BRG1 is a core component of the BAF-complex through all stages of neural maturation, and its mRNA transcript was not observed to be an ethanol target (Figure 1). Therefore, prior to targeting BRG1 for chromatin immuno-precipitation studies, we assessed its sub-cellular compartmentalization by western immunoblot assay, and, additionally, assessed whether ethanol regulated BRG1 protein. A single BRG1 immunoreactive band was observed at 238 kD in the nuclear but not cytoplasmic fraction from neurosphere cultures (Figure 3a), corresponding to the expected molecular weight of the protein. This indicates that any BRG1-containing complex is likely to be predominantly nuclear in location. Moreover, ethanol exposure did not significantly alter BRG1 protein ($F_{(2,6)}$=0.52, p<0.62, Figure 3b,c), consistent with the data obtained for BRG1 mRNA. These data indicate that any ethanol-induced change in BRG1-containing complexes is unlikely to be due to a change in BRG1 expression. Finally, BRG1 was specifically and efficiently immuno-precipitated from the nuclear but not cytoplasmic fraction by the anti-BRG-1 antibody (Figure 3d), and therefore, the anti-BRG1 antibody was used for chromatin immunoprecipitation (ChIP) analyses.

We selected 6 regions of the pri-miR-9-2 gene locus to assess BRG1 binding based on their position relative to ENCODE project identified binding sites for factors c-myc and Oct4/Pou5f1, which promote stem cell renewal and pluripotency, for the inhibitor of differentiation, REST (neuron-RESTrictive silencer factor) Figure 4a), as well as a site

within the pre-miR-9-2 encoding region. BRG1 ChIP analysis showed that the pre-miR-9-2 region as well as pri-miR-9-2 regions 1,2,3,4 and 5 all exhibited BRG1 binding at a significantly higher level than that observed at a gene desert located on Chr6qC3 (Figure 4b, pairwise comparisons, all p's<0.02 for four independent replicate experiments). The DNAse I hypersensitivity assay indicated that regions encoding pre-miR-9-2 pri-miR-9-2 regions 1,2,4 and 5 were all within DNAse I hypersensitive regions of pri-miR-9-2. Region 3, however, was resistant to DNAse I digestion, as would be predicted from its location within an identified CpG island (Figure 4c, data from two independent replicates). These data indicate that BRG1 containing complexes bind to both DNAse I hypersensitive and resistant regions of the pri-miR-9-2 coding region.

Ethanol exposure specifically increases BRG1 binding to the pre-miR-9-2 coding region

Control neurosphere cultures, or cultures treated with ethanol (120mg/dl for 5 days, 5 independent replicate experiments), were assessed for BRG1 binding to pri-miR-9-2 regions 1 to 5, and the pre-miR-9-2 coding exon (as schematized in Figure 4a). Overall, multivariate analysis showed a significant global effect of ethanol exposure on BRG1 binding (Pillai's trace statistic, $F_{(6,3)}$=11.38, p<0.036). Post-hoc univariate analysis showed that ethanol resulted in a significant ~3-fold increase in BRG1 binding specifically within region 3, which contains a CpG island ($F_{(1,8)}$=24.48, p<0.001, Figure 5), and the pre-miR-9-2 coding exon ($F_{(1,8)}$=9.55, p<0.015, Figure 5), but not within regions 1, 2, 4 and 5 (all p's>0.19). In comparison, little BRG1 binding was observed to the control Chr6:qC3 locus (Figure 5, gray bar).

Disruption of the BAF complex results in a decrease in miR-9 in NSCs

BAF155 and BAF170 are core components of the neuronal lineage-specific Baf (nBAF) complex (Ho and Crabtree, 2010), and simultaneous knockdown of both BAF155 and BAF170 have been shown to be effective in inactivating the BAF complex (Nguyen et al., 2016). We therefore used siRNAs to simultaneously knockdown both BAF155 and 170, to disrupt the BAF complex. Controls included scrambled siRNAs and siRNAs targeted to cyclophilin-B (Peptidylprolyl Isomerase B, PPIB), a common endoplasmic reticulum-associated protein found in all cell-types (Price et al., 1991). BAF155/BAF170 siRNA mixtures resulted in a significant suppression of both the BAF155 and BAF170 transcripts but not cyclophilin-B (Figure 6a, all p's< 0.001), and conversely, cyclophilin-B siRNA significantly decreased cyclophilin B mRNA (p< 0.001), but did not alter BAF155 or BAF170 mRNA levels (Figure 6b). In comparison to the scrambled siRNA control, siRNAs to BAF155/BAF170 result in a significant, ~50% decrease in miR-9 expression (paired t-test, p<0.015, n=8 sample pairs). In contrast, cyclophilin-B siRNA resulted in a marginal, but not statistically significant increase (paired t-test, p<0.09, n=5 sample pairs) in miR-9 (Figure 6c).

Discussion

MiR-9 is among the most highly expressed miRNAs in fetal brain during the fetal neurogenic period (Miranda, 2014), and plays an important role in early brain segmentation, neurogenesis and neuronal maturation (Leucht et al., 2008; Shibata et al., 2008; Shibata et

al., 2011). MiR-9 is also likely to be an important mediator of the effects of PAE, since ethanol exposure results in a loss of brain miR-9 and loss of miR-9 in turn, in zebrafish models, mimics craniofacial (Pappalardo-Carter et al., 2013) and behavioral (Tal et al., 2012) phenotypes associated with heavy PAE. Of the three unique primary transcripts, pri-miR-9-1, −2 and −3 (on mouse chromosomes 3, 13 and 7, respectively), that encode mature mammalian miR-9, pri-miR-9-2 (ENSMUST00000131907/ C130071C03Rik) was specifically found to be an epigenetic target of ethanol in mouse NSCs, in that heavy exposure, at levels associated with excessive alcohol consumption in human populations (Adachi et al., 1991), resulted in increased methylation at this locus (Pappalardo-Carter et al., 2013).

The SWI/SNF/BAF-complex functions as an antagonist to DNA methylation machinery, as a means to disassemble nucleosomes and unpack chromatin (Kadoch et al., 2016). The SWI/SNF complex has been shown to generally facilitate transcription (Neely et al., 1999; Yudkovsky et al., 1999), but may also mediate direct transcription repression in yeast (Sudarsanam et al., 2000), and the BAF complex may have similar bi-functional effects in mammalian stem cells (Zhang et al., 2014). In the current study, ChIP analysis indicated that BRG1 could bind to both DNAse I hypersensitive and resistant sites, suggesting that the BAF complex associates with both euchromatic (transcriptionally assessable) and heterochromatic methylated CpG islands within the pri-miR-9-2 locus. Moreover, combinational knockdown of BAF155 and BAF170, which is required for BAF-complex dissolution (Nguyen et al., 2016), resulted in approximately 50% reduction in miR-9. This outcome supports a model for the BAF-complex as means for increasing chromatin accessibility to promote miR-9 gene transcription. The BAF complex has also been shown to promote activation of the pluripotency maintenance transcription factor Oct4/Pou5F1 in somatic cells to facilitate their transformation to stem cells (Singhal et al., 2010). However, ethanol exposure did not increase binding of BRG1 to probed regions 1 and 4 of the pri-miR-9-2 locus which contained identified Oct4/Pou5f1 binding sites. This result is consistent with our previous data showing that ethanol exposure results in an overall loss of stem cell capacity in fetal neural epithelial cells (Santillano et al., 2005; Tingling et al., 2013).

A previous study showed that at least one member of the BAF complex, SMARCA2 (BAF190B) was methylated in NSCs following ethanol exposure (Zhou et al., 2011), a result that is consistent with epigenetic silencing of miR-9-2. It was therefore surprising, and contrary to our predictions, to observe that ethanol exposure resulted in an increased expression of BAF complex transcripts, particularly, those transcripts that were specific constituents for the neural progenitor (np) and neuronal (n)BAF-complexes. Moreover, ethanol exposure resulted in a significant increase in the association of BRG1 with chromatin within the exon encoding pre-miR-9-2 and within the DNAse I resistant pri-miR-9-2 domain 3, which is predicted to contain a CpG island. The functional consequences of a selective increase in Brg-complex binding within these regions are unknown. However, it is possible that the ethanol-induced increase in Brg-complex association with the pre-miR-9-2 exon and the CpG-island containing domain constitutes a protective, anti-teratogenic developmental adaptation to protect against a complete loss of a miRNA that is particularly critical for early brain development.

The mechanisms underlying a compensatory developmental adaptation of the BAF-complex are also unknown. However, the presence of a miR-9 – BAF-complex regulatory feedback loop may partly explain the increased BRG1 binding to the pre-miR-9-2 coding exon. Other research groups have shown that miR-9* (miR-9-3p / the passenger strand miRNA) targets BAF53a for translational repression by binding to the 3'-UTR of its mRNA (Yoo et al., 2009). BAF53a is a component of the npBAF-complex, and therefore, the loss of miR-9 following ethanol exposure may stabilize npBAF-complexes and maintain their functional capacity to continue to facilitate progenitor maturation by minimizing the effect of ethanol on miR-9.

The BAF complex (Nguyen et al., 2016) and miR-9 (Pappalardo-Carter et al., 2013) are both important for promoting brain growth. Our data further indicate that the BAF-complex is an epigenetic regulator of the pri-miR-9-2 locus at least, in an ex vivo model for fetal NSCs. The observed increased binding of BRG1 to the pre-miR-9-2 encoding exon and to CpG-island containing introns following ethanol exposure is particularly important. Given the role of the BAF complex in nucleosome dis-assembly and as a facilitator of gene transcription, it is possible that this complex may serve to prevent a complete loss of transcription from the miR-9-2 locus following ethanol exposure. It will be important in future studies to assess the compensatory role of the BAF-complex *in vivo*, in whole animal models of PAE. However, these findings support the possibility that fetal NSCs may adaptively recruit resiliency factors to diminish adverse effects of teratogens like ethanol.

Acknowledgments

References

Adachi J, Mizoi Y, Fukunaga T, Ogawa Y, Ueno Y, Imamichi H. Degrees of alcohol intoxication in 117 hospitalized cases. J Stud Alcohol. 1991; 52(5):448–453. [PubMed: 1943100]

Balaraman S, Winzer-Serhan UH, Miranda RC. Opposing actions of ethanol and nicotine on microRNAs are mediated by nicotinic acetylcholine receptors in fetal cerebral cortical-derived neural progenitor cells. Alcohol Clin Exp Res. 2012; 36(10):1669–77. [PubMed: 22458409]

Bultman S, Gebuhr T, Yee D, La Mantia C, Nicholson J, Gilliam A, Randazzo F, Metzger D, Chambon P, Crabtree G, Magnuson T. A Brg1 null mutation in the mouse reveals functional differences among mammalian SWI/SNF complexes. Mol Cell. 2000; 6(6):1287–95. [PubMed: 11163203]

Bystron I, Blakemore C, Rakic P. Development of the human cerebral cortex: Boulder Committee revisited. Nat Rev Neurosci. 2008; 9(2):110–22. [PubMed: 18209730]

Camarillo C, Miranda RC. Ethanol exposure during neurogenesis induces persistent effects on neural maturation: evidence from an ex vivo model of fetal cerebral cortical neuroepithelial progenitor maturation. Gene Expr. 2008; 14(3):159–71. [PubMed: 18590052]

Finer LB, Zolna MR. Declines in Unintended Pregnancy in the United States, 2008–2011. N Engl J Med. 2016; 374(9):843–52. [PubMed: 26962904]

Follows GA, Janes ME, Vallier L, Green AR, Gottgens B. Real-time PCR mapping of DNaseI-hypersensitive sites using a novel ligation-mediated amplification technique. Nucleic Acids Res. 2007; 35(8):e56. [PubMed: 17389645]

Ho L, Crabtree GR. Chromatin remodelling during development. Nature. 2010; 463(7280):474–84. [PubMed: 20110991]

Jones KL, Smith DW, Ulleland CN, Streissguth P. Pattern of malformation in offspring of chronic alcoholic mothers. Lancet. 1973; 1(7815):1267–71. [PubMed: 4126070]

Kadoch C, Copeland RA, Keilhack H. PRC2 and SWI/SNF Chromatin Remodeling Complexes in Health and Disease. Biochemistry. 2016; 55(11):1600–14. [PubMed: 26836503]

Kent WJ, Sugnet CW, Furey TS, Roskin KM, Pringle TH, Zahler AM, Haussler D. The human genome browser at UCSC. Genome Res. 2002; 12(6):996–1006. [PubMed: 12045153]

Kosho T, Okamoto N. Genotype-phenotype correlation of Coffin-Siris syndrome caused by mutations in SMARCB1, SMARCA4, SMARCE1, and ARID1A. Am J Med Genet C Semin Med Genet. 2014; 166(3):262–75.

Laufer BI, Kapalanga J, Castellani CA, Diehl EJ, Yan L, Singh SM. Associative DNA methylation changes in children with prenatal alcohol exposure. Epigenomics. 2015; 7(8):1259–74. [PubMed: 26178076]

Lemoine P, Harouseau H, Borteryu JT, Menuet JC. Les enfants des parents alcooliques: Anomalies observees apropos de 127 cas. Ouest Medical. 1968; 21:476–482.

Lessard J, Wu JI, Ranish JA, Wan M, Winslow MM, Staahl BT, Wu H, Aebersold R, Graef IA, Crabtree GR. An essential switch in subunit composition of a chromatin remodeling complex during neural development. Neuron. 2007; 55(2):201–15. [PubMed: 17640523]

Leucht C, Stigloher C, Wizenmann A, Klafke R, Folchert A, Bally-Cuif L. MicroRNA-9 directs late organizer activity of the midbrain-hindbrain boundary. Nat Neurosci. 2008; 11(6):641–8. [PubMed: 18454145]

Liu Y, Balaraman Y, Wang G, Nephew KP, Zhou FC. Alcohol exposure alters DNA methylation profiles in mouse embryos at early neurulation. Epigenetics. 2009; 4(7):500–11. [PubMed: 20009564]

Maier SE, Miller JA, West JR. Prenatal binge-like alcohol exposure in the rat results in region-specific deficits in brain growth. Neurotoxicol Teratol. 1999; 21(3):285–91. [PubMed: 10386832]

Masemola ML, van der Merwe L, Lombard Z, Viljoen D, Ramsay M. Reduced DNA methylation at the PEG3 DMR and KvDMR1 loci in children exposed to alcohol in utero: a South African Fetal Alcohol Syndrome cohort study. Front Genet. 2015; 6:85. [PubMed: 25806045]

Mathies LD, Blackwell GG, Austin MK, Edwards AC, Riley BP, Davies AG, Bettinger JC. SWI/SNF chromatin remodeling regulates alcohol response behaviors in Caenorhabditis elegans and is associated with alcohol dependence in humans. Proc Natl Acad Sci U S A. 2015; 112(10):3032–7. [PubMed: 25713357]

Miller M. Effects of prenatal exposure to ethanol on neocortical development: II. Cell proliferation in the ventricular and subventricular zones of the rat. The Journal of Comparative Neurology. 1989; 287:326–338. [PubMed: 2778108]

Miller MW, Nowakowski RS. Effect of prenatal exposure to ethanol on the cell cycle kinetics and growth fraction in the proliferative zones of fetal rat cerebral cortex. Alcohol Clin Exp Res. 1991; 15(2):229–32. [PubMed: 2058800]

Miranda RC. MicroRNAs and Ethanol Toxicity. Int Rev Neurobiol. 2014; 115:245–84. [PubMed: 25131547]

Miranda RC, Santillano DR, Camarillo C, Dohrman D. Modeling the impact of alcohol on cortical development in a dish: strategies from mapping neural stem cell fate. Methods Mol Biol. 2008; 447:151–68. [PubMed: 18369918]

Neely KE, Hassan AH, Wallberg AE, Steger DJ, Cairns BR, Wright AP, Workman JL. Activation domain-mediated targeting of the SWI/SNF complex to promoters stimulates transcription from nucleosome arrays. Mol Cell. 1999; 4(4):649–55. [PubMed: 10549297]

Nguyen H, Sokpor G, Pham L, Rosenbusch J, Stoykova A, Staiger JF, Tuoc T. Epigenetic regulation by BAF (mSWI/SNF) chromatin remodeling complexes is indispensable for embryonic development. Cell Cycle. 2016; 15(10):1317–24. [PubMed: 26986003]

Pappalardo-Carter DL, Balaraman S, Sathyan P, Carter ES, Chen WJ, Miranda RC. Suppression and epigenetic regulation of MiR-9 contributes to ethanol teratology: evidence from zebrafish and murine fetal neural stem cell models. Alcohol Clin Exp Res. 2013; 37(10):1657–67. [PubMed: 23800254]

Pietrzykowski AZ, Friesen RM, Martin GE, Puig SI, Nowak CL, Wynne PM, Siegelmann HT, Treistman SN. Posttranscriptional regulation of BK channel splice variant stability by miR-9 underlies neuroadaptation to alcohol. Neuron. 2008; 59(2):274–87. [PubMed: 18667155]

Portales-Casamar E, Lussier AA, Jones MJ, MacIsaac JL, Edgar RD, Mah SM, Barhdadi A, Provost S, Lemieux-Perreault LP, Cynader MS, Chudley AE, Dube MP, Reynolds JN, Pavlidis P, Kobor MS. DNA methylation signature of human fetal alcohol spectrum disorder. Epigenetics Chromatin. 2016; 9:25. [PubMed: 27358653]

Price ER, Zydowsky LD, Jin MJ, Baker CH, McKeon FD, Walsh CT. Human cyclophilin B: a second cyclophilin gene encodes a peptidyl-prolyl isomerase with a signal sequence. Proc Natl Acad Sci U S A. 1991; 88(5):1903–7. [PubMed: 2000394]

Prock TL, Miranda RC. Embryonic cerebral cortical progenitors are resistant to apoptosis, but increase expression of suicide receptor DISC-complex genes and suppress autophagy following ethanol exposure. Alcohol Clin Exp Res. 2007; 31(4):694–703. [PubMed: 17374049]

Roozen S, Peters GJ, Kok G, Townend D, Nijhuis J, Curfs L. Worldwide Prevalence of Fetal Alcohol Spectrum Disorders: A Systematic Literature Review Including Meta-Analysis. Alcohol Clin Exp Res. 2016; 40(1):18–32. [PubMed: 26727519]

Santillano DR, Kumar LS, Prock TL, Camarillo C, Tingling JD, Miranda RC. Ethanol induces cell-cycle activity and reduces stem cell diversity to alter both regenerative capacity and differentiation potential of cerebral cortical neuroepithelial precursors. BMC Neurosci. 2005; 6:59. [PubMed: 16159388]

Sathyan P, Golden HB, Miranda RC. Competing interactions between micro-RNAs determine neural progenitor survival and proliferation after ethanol exposure: evidence from an ex vivo model of the fetal cerebral cortical neuroepithelium. J Neurosci. 2007; 27(32):8546–57. [PubMed: 17687032]

Shibata M, Kurokawa D, Nakao H, Ohmura T, Aizawa S. MicroRNA-9 Modulates Cajal-Retzius Cell Differentiation by Suppressing Foxg1 Expression in Mouse Medial Pallium. J. Neurosci. 2008; 28(41):10415–10421. [PubMed: 18842901]

Shibata M, Nakao H, Kiyonari H, Abe T, Aizawa S. MicroRNA-9 regulates neurogenesis in mouse telencephalon by targeting multiple transcription factors. J Neurosci. 2011; 31(9):3407–22. [PubMed: 21368052]

Singhal N, Graumann J, Wu G, Arauzo-Bravo MJ, Han DW, Greber B, Gentile L, Mann M, Scholer HR. Chromatin-Remodeling Components of the BAF Complex Facilitate Reprogramming. Cell. 2010; 141(6):943–55. [PubMed: 20550931]

Sudarsanam P, Iyer VR, Brown PO, Winston F. Whole-genome expression analysis of snf/swi mutants of Saccharomyces cerevisiae. Proc Natl Acad Sci U S A. 2000; 97(7):3364–9. [PubMed: 10725359]

Sudheendran N, Bake S, Miranda RC, Larin KV. Comparative assessments of the effects of alcohol exposure on fetal brain development using optical coherence tomography and ultrasound imaging. J Biomed Opt. 2013; 18(2):20506. [PubMed: 23386196]

Tal TL, Franzosa JA, Tilton SC, Philbrick KA, Iwaniec UT, Turner RT, Waters KM, Tanguay RL. MicroRNAs control neurobehavioral development and function in zebrafish. FASEB J. 2012; 26(4):1452–1461. [PubMed: 22253472]

Tan CH, Denny CH, Cheal NE, Sniezek JE, Kanny D. Alcohol use and binge drinking among women of childbearing age - United States, 2011–2013. MMWR Morb Mortal Wkly Rep. 2015; 64(37): 1042–6. [PubMed: 26401713]

Tingling JD, Bake S, Holgate R, Rawlings J, Nagsuk PP, Chandrasekharan J, Schneider SL, Miranda RC. CD24 expression identifies teratogen-sensitive fetal neural stem cell subpopulations: evidence from developmental ethanol exposure and orthotopic cell transfer models. PLoS One. 2013; 8(7):e69560. [PubMed: 23894503]

Tsai PC, Bake S, Balaraman S, Rawlings J, Holgate RR, Dubois D, Miranda RC. MiR-153 targets the nuclear factor-1 family and protects against teratogenic effects of ethanol exposure in fetal neural stem cells. Biol Open. 2014; 3(8):741–58. [PubMed: 25063196]

Van Houdt JK, Nowakowska BA, Sousa SB, van Schaik BD, Seuntjens E, Avonce N, Sifrim A, Abdul-Rahman OA, van den Boogaard MJ, Bottani A, Castori M, Cormier-Daire V, Deardorff MA, Filges I, Fryer A, Fryns JP, Gana S, Garavelli L, Gillessen-Kaesbach G, Hall BD, Horn D, Huylebroeck

Author Manuscript

Author Manuscript

Author Manuscript

Author Manuscript

D, Klapecki J, Krajewska-Walasek M, Kuechler A, Lines MA, Maas S, Macdermot KD, McKee S, Magee A, de Man SA, Moreau Y, Morice-Picard F, Obersztyn E, Pilch J, Rosser E, Shannon N, Stolte-Dijkstra I, Van Dijck P, Vilain C, Vogels A, Wakeling E, Wieczorek D, Wilson L, Zuffardi O, van Kampen AH, Devriendt K, Hennekam R, Vermeesch JR. Heterozygous missense mutations in SMARCA2 cause Nicolaides-Baraitser syndrome. Nat Genet. 2012; 44(4):445–9. S1. [PubMed: 22366787]

Veazey KJ, Carnahan MN, Muller D, Miranda RC, Golding MC. Alcohol-induced epigenetic alterations to developmentally crucial genes regulating neural stemness and differentiation. Alcohol Clin Exp Res. 2013; 37(7):1111–22. [PubMed: 23488822]

Veazey KJ, Parnell SE, Miranda RC, Golding MC. Dose-dependent alcohol-induced alterations in chromatin structure persist beyond the window of exposure and correlate with fetal alcohol syndrome birth defects. Epigenetics Chromatin. 2015; 8(1):39. [PubMed: 26421061]

Vogel-Ciernia A, Wood MA. Neuron-specific chromatin remodeling: a missing link in epigenetic mechanisms underlying synaptic plasticity, memory, and intellectual disability disorders. Neuropharmacology. 2014; 80:18–27. [PubMed: 24140580]

Ye J, Coulouris G, Zaretskaya I, Cutcutache I, Rozen S, Madden TL. Primer-BLAST: a tool to design target-specific primers for polymerase chain reaction. BMC Bioinformatics. 2012; 13:134. [PubMed: 22708584]

Yoo AS, Staahl BT, Chen L, Crabtree GR. MicroRNA-mediated switching of chromatin-remodelling complexes in neural development. Nature. 2009; 460(7255):642–6. [PubMed: 19561591]

Yudkovsky N, Logie C, Hahn S, Peterson CL. Recruitment of the SWI/SNF chromatin remodeling complex by transcriptional activators. Genes Dev. 1999; 13(18):2369–74. [PubMed: 10500094]

Zhang X, Li B, Li W, Ma L, Zheng D, Li L, Yang W, Chu M, Chen W, Mailman RB, Zhu J, Fan G, Archer TK, Wang Y. Transcriptional repression by the BRG1-SWI/SNF complex affects the pluripotency of human embryonic stem cells. Stem Cell Reports. 2014; 3(3):460–74. [PubMed: 25241744]

Zhou FC, Balaraman Y, Teng M, Liu Y, Singh RP, Nephew KP. Alcohol alters DNA methylation patterns and inhibits neural stem cell differentiation. Alcohol Clin Exp Res. 2011; 35(4):735–46. [PubMed: 21223309]

Highlights

- The miR-9-2 gene locus is an epigenetic target of ethanol in fetal neural stem cells.

- The BAF-complex associates with the pri-miR-9-2 gene locus.

- The BAF-complex promotes miR-9 expression.

- Ethanol increases BAF complex component expression

- Ethanol promotes BAF-complex binding to the pri-miR-9-2 locus.

- The BAF-complex may be a resiliency factor that protects miR-9-2 from ethanol.
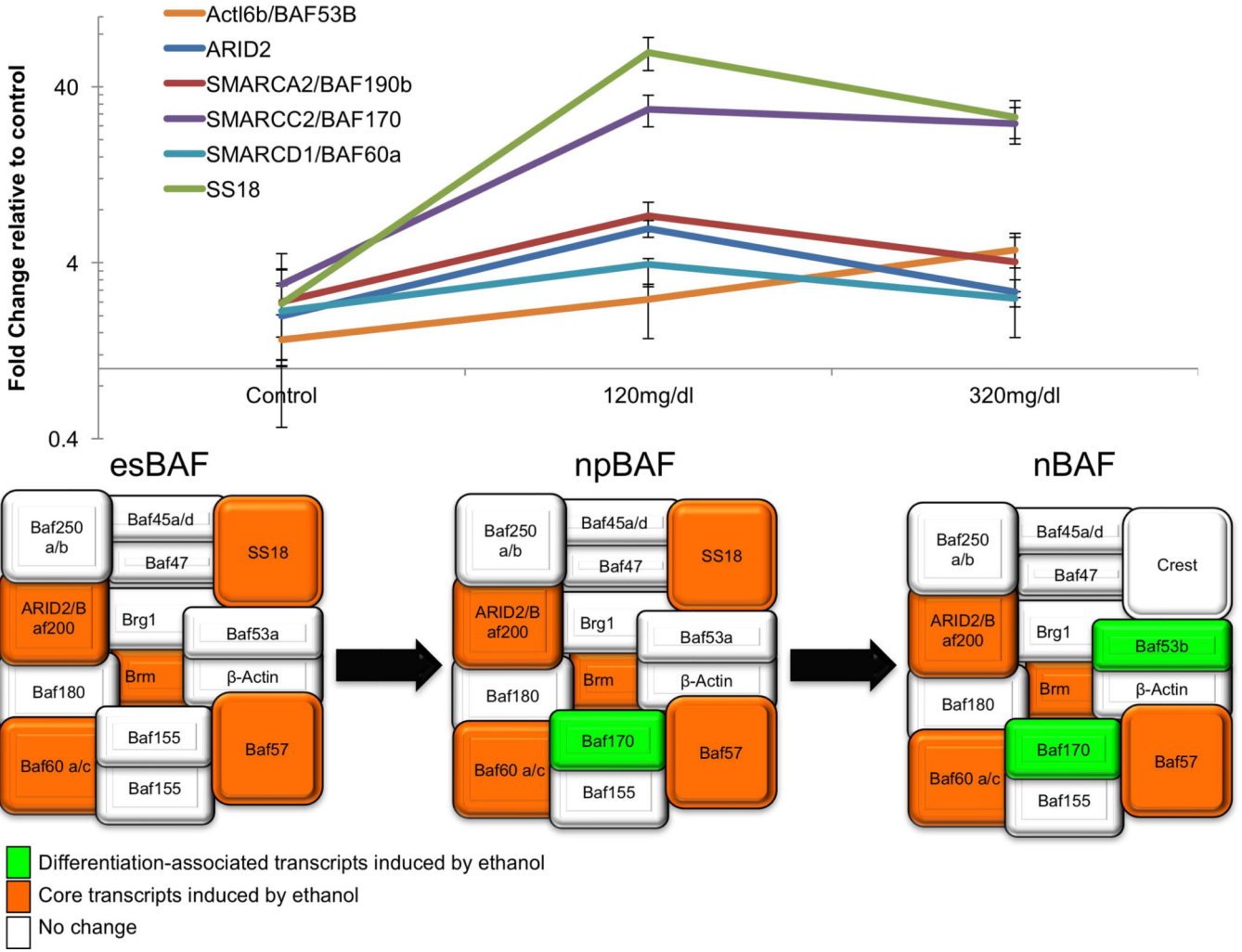
Figure 1. Specific BAF complex subunit transcripts are induced in NSCs following ethanol exposure

(a) mRNA levels of BAF subunits in neurospheres after 120mg/dl and 320mg/dl ethanol treatment calculated as fold change normalized to control (0mg/dl ethanol). Error bars shows standard error of the mean. (b) Schematic diagram shows the components of the BAF complex in embryonic stem cells (esBAF), neural progenitor cells (npBAF) and in neurons (nBAF). Orange color indicates the subunits which are maintained in different cell maturation stages from embryonic stem cells state through the differentiation and whose mRNA levels were induced by ethanol treatment. Green color indicates subunits which are exclusively found in the BAF complex in differentiated neuronal states, and whose mRNA levels were induced by ethanol treatment. White color indicates the subunits whose mRNA levels were not affected by ethanol.
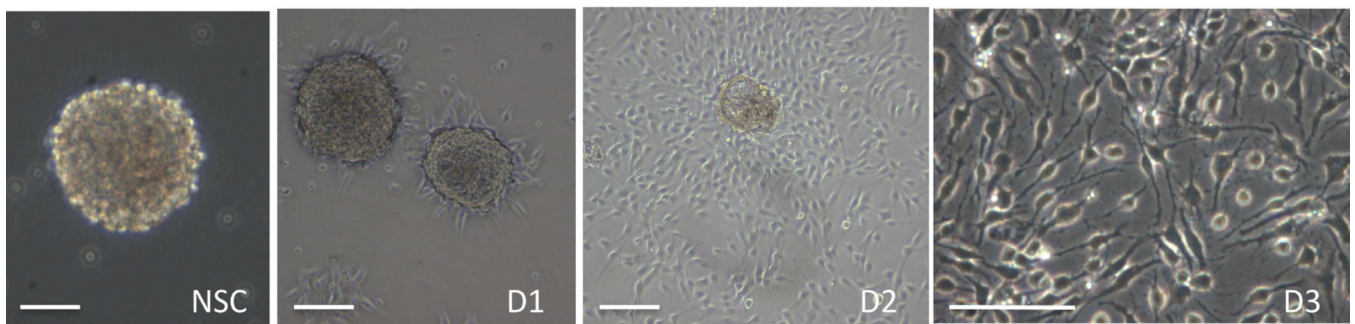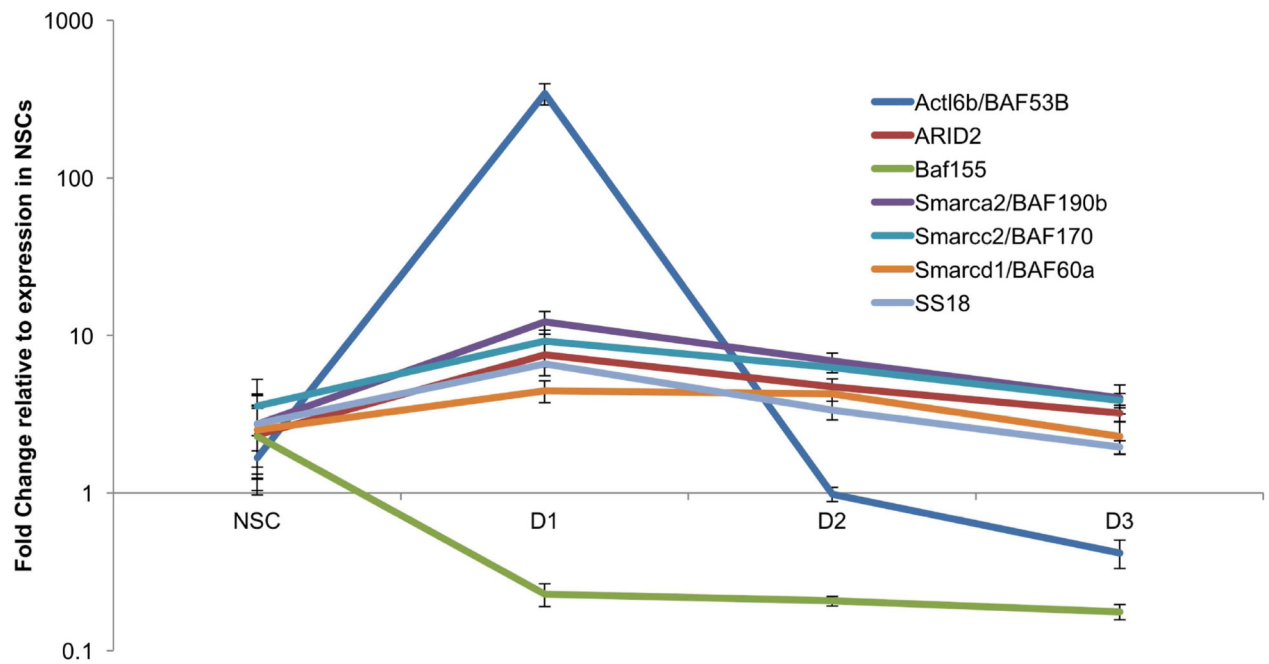
Figure 2. Ethanol-sensitive BAF complex transcripts are transiently induced during neural differentiation

(a) BAF complex subunit expression over a three-day course of mitogen withdrawal, BDNF-induced neural differentiation calculated as fold change normalized to expression in NSCs (Day 0). Error bars show standard error of the mean. (b) Phase contrast microscopy of a neurosphere (left) and cells over three days (D1, D2 and D3) of neural differentiation. Scale bar, 100 μm.
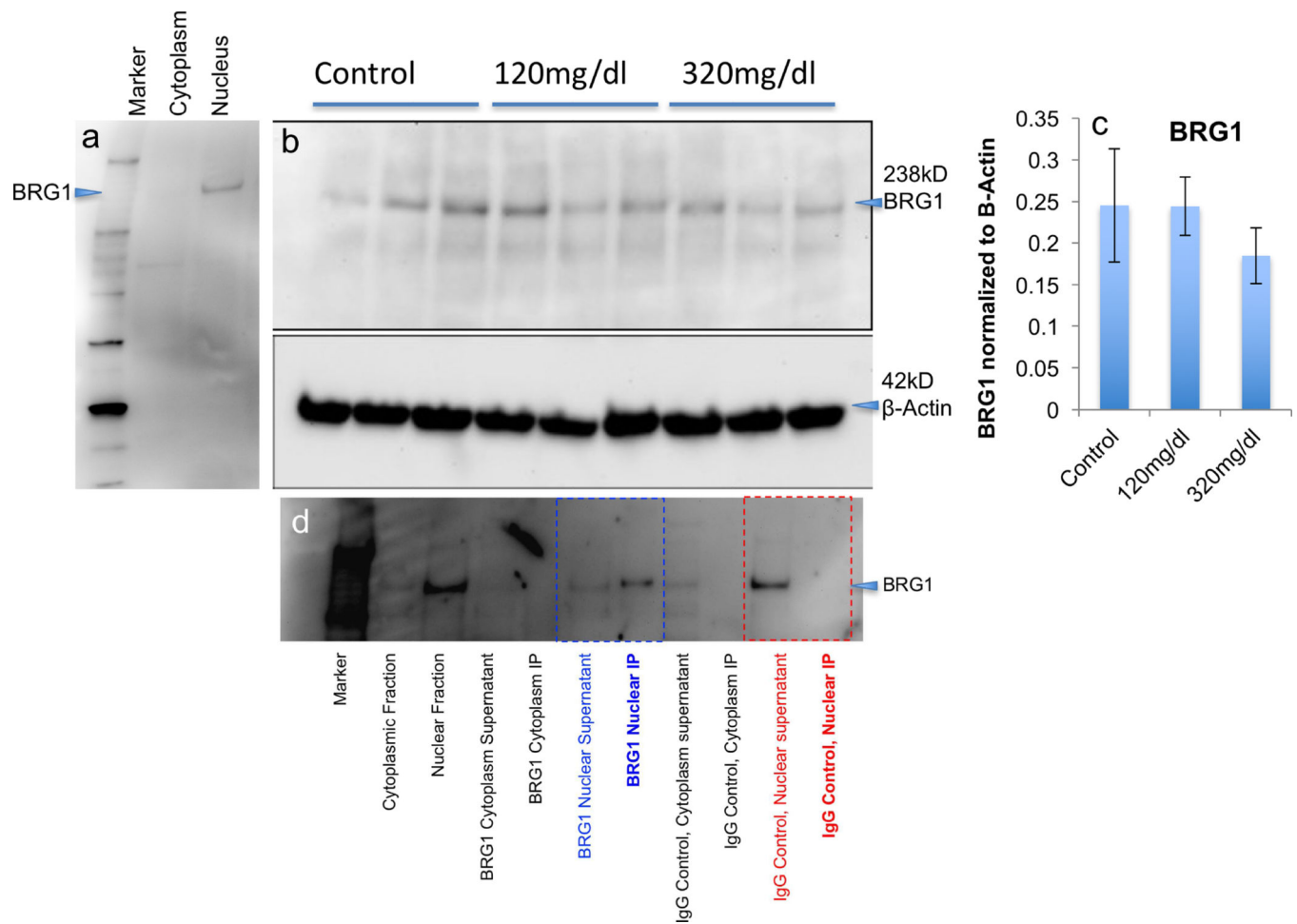
Figure 3. BRG1 protein expression in NSCs

(a) Western immunoblot shows a single BRG1 band at ~238KD detected in the nuclear extract of neurosphere cultures but not in the cytoplasmic extract. (b) BRG1 protein levels in neurospheres after 0mg/dl, 120mg/dl and 320mg/dl ethanol treatment. Lower panel shows the corresponding immunoblot when probed for β-Actin as a loading control. (c) Bar graph, depicting the quantification of the western blot, shows that ethanol did not alter BRG1 protein expression, consistent with the lack of effect on BRG1 mRNA expression. The vertical axis shows the ratio of the band density of BRG1 to the ratio of the band density of β-Actin. Error bars indicates standard error of the mean. (d) Western blot analysis of BRG1 immunoprecipitation in cytoplasmic and nuclear cellular fractions probed with anti-BRG1 antibody. BRG1 is specifically precipitated with anti-BRG1 antibody (blue text), but not with an isotype-specific IgG control antibody (red text). Efficiency of anti-BRG1 immunoprecipitation is indicated by the relative depletion of BRG1 from the nuclear supernatant and enrichment in the immuno-precipitate (IP).
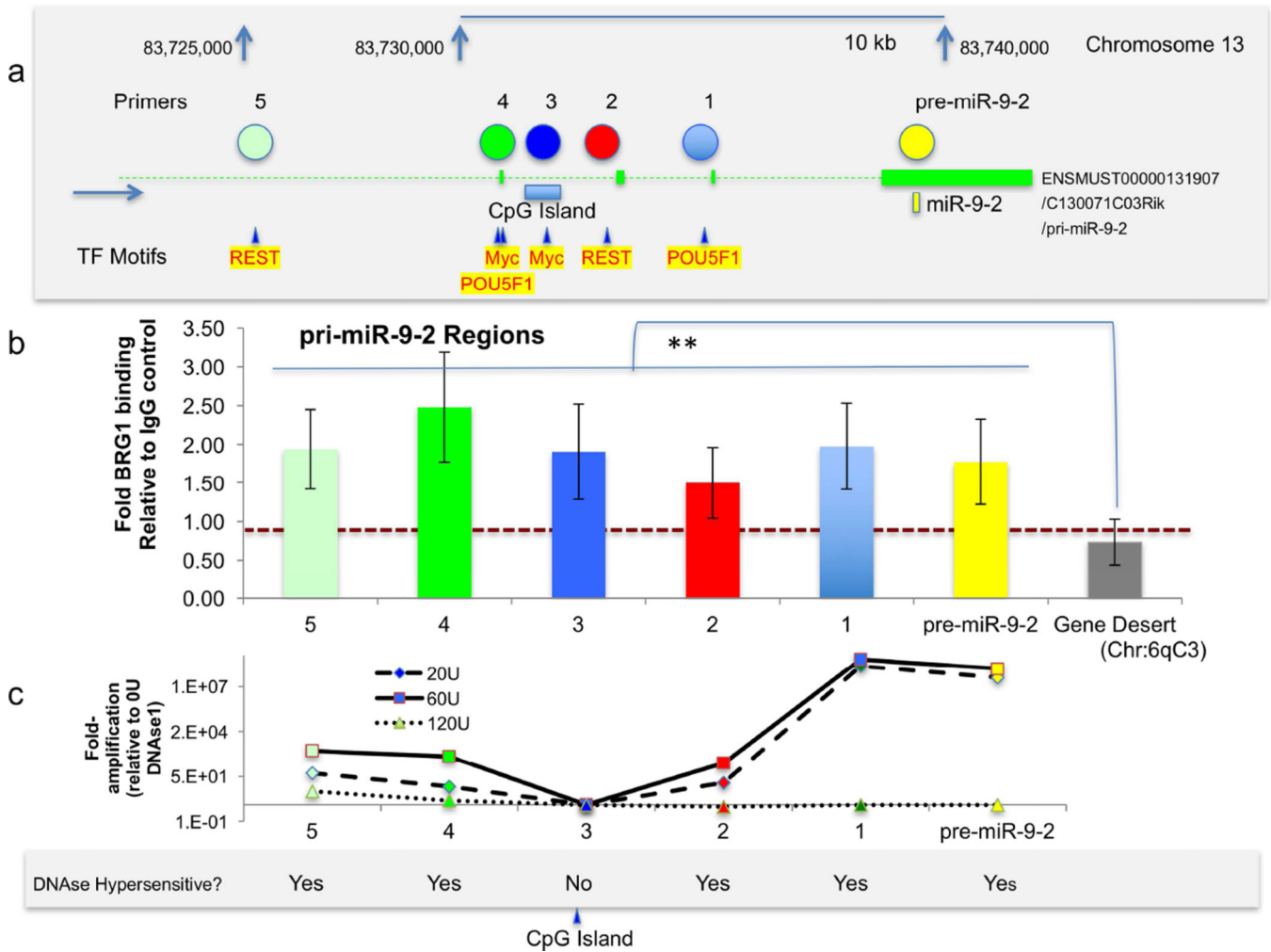
Figure 4. BRG1-containing complexes associate with both DNAse I-hypersensitive and insensitive sites on the miR-9-2 gene locus

(a) Positional representation of POU5F1/Oct4, c-myc and REST transcription regulatory factor binding sites along the human pre-miR-9-2 gene locus identified with the UCSC genome browser ENCODE analysis hub track. Colored circles indicate locations for primer pairs for pri-miR-9-2 regions 1,2,3,4 and 5 and the pre-miR-9-2 coding region. (b) qPCR results of BRG1-ChIP from neurospheres. Primers were used to amplify 6 distinct positions along the pri-miR-9-2 gene locus and a genetically sparse region on mouse chromosome 6. Vertical axis shows fold change relative to an IgG pulldown control. Error bars indicate standard error of the mean. (c) qPCR of neurosphere DNA following digestion with 20, 60 and 120U of DNAse I at the 6 positions along the pri-miR-9-2 gene locus. The vertical axis shows fold amplification relative to DNAse I-untreated neurosphere DNA.
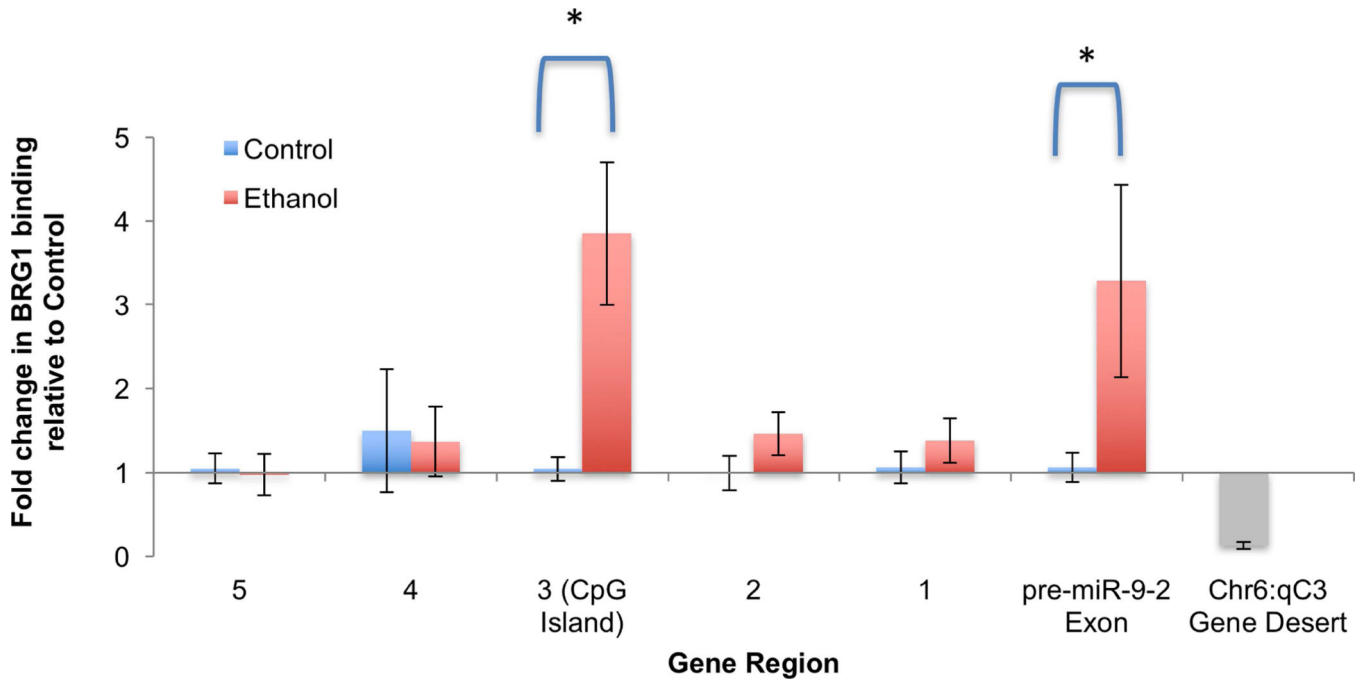
Figure 5. ChIP analysis indicates that ethanol exposure increases BRG1 binding to DNAse I-resistant/CpG island containing region 3 and the pre-miR-9-2 coding exon

Bar graph shows the effect of ethanol on BRG1-association with regions 1 to 5 and the pre-miR-9-2 exon-coding region of the primary (pri)-miR-9-2 coding locus. Primers for a gene desert on chromosome 6 (not predicted to bind any transcription factors) shows the specificity of the immuno-precipitation. Vertical axis shows the fold change of the specific associated DNA region to BRG1 in ethanol treated group relative to control group. Error bars indicate standard error of the mean.
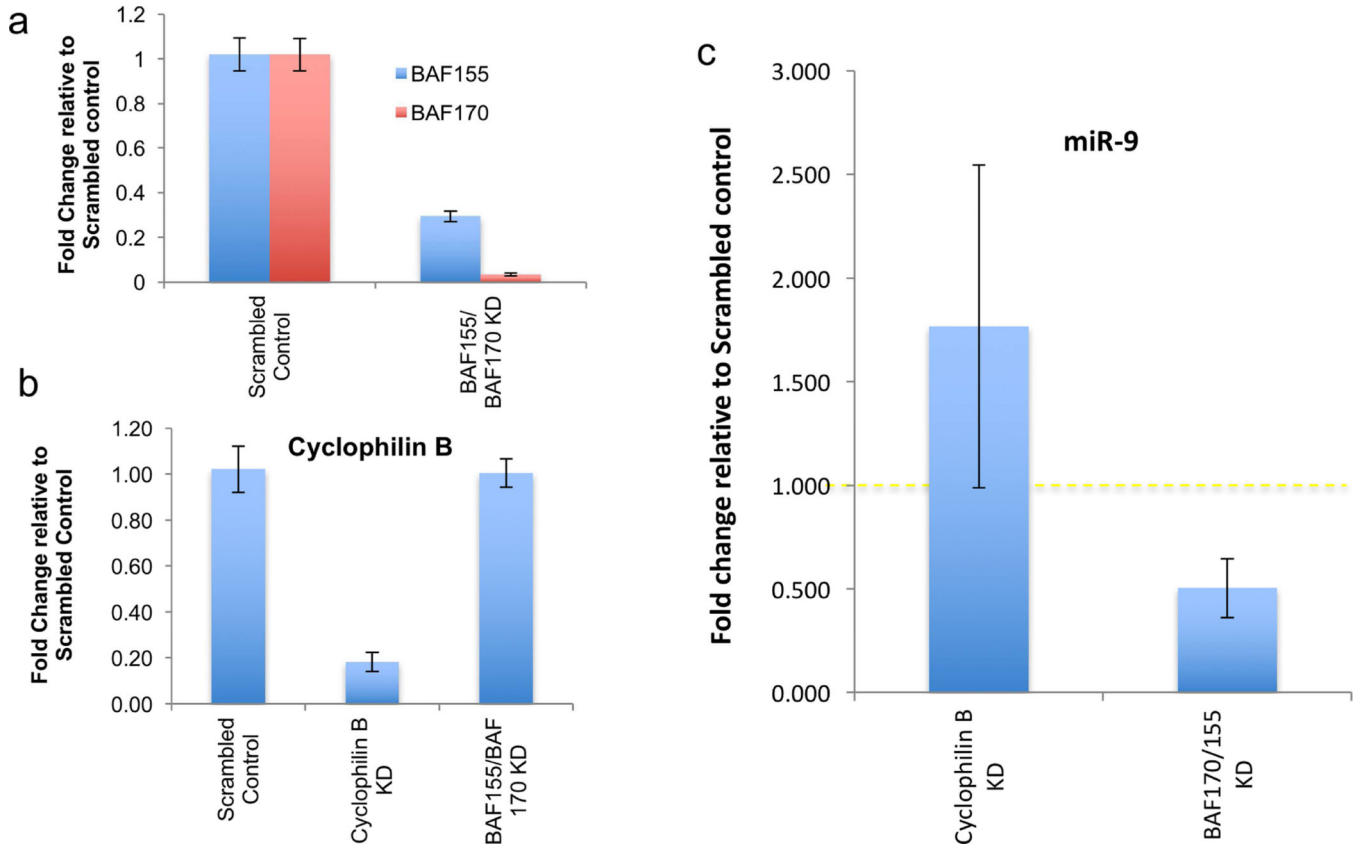
Figure 6. siRNA mediated BAF155 and BAF 170 knockdown results in specific downregulation of miR-9

(a) Levels of BAF155 and BAF170 mRNA after BAF155/BAF-170 knockdown, normalized to β-Actin mRNA expression levels and calculated as fold change relative to scrambled siRNA control group. (b) Cyclophilin-B mRNA level after either scrambled siRNA, cyclophilin-B siRNA or combined BAF155/BAF170 siRNA transfection, normalized to β-Actin mRNA expression levels and calculated as fold change relative to scrambled control. (c) mir-9 levels measured by qRT-PCR normalized to U6 snRNA expression levels and calculated as fold-change relative to control scrambled siRNA transfected group. BAF155/170 knockdown resulted in a significant decrease in miR-9. However, cyclophilin-D knockdown did not result in altered miR-9 expression. Error bars indicate standard error of the mean.

Table 1

Primer Constructs

Hugo nomenclature	Synonyms		Primers (5'-3')	Product size	NCBI Accession number	sequence verified
SMARCE1	BAF57	Fwd:	AGGCTTCCAACCCTGACCTA	478	NM_020618.4	yes
		Rev:	TCGGCTTCTAGTTTCCGCTG			
SMARCC2	BAF170	Fwd:	GAACCGCCAACCAACAAGTC	578	NM_001114097.1	yes
		Rev:	GGTTTCTCAGGAGTGGGAGC			
SS18	SYT	Fwd:	CCACCTCCACAGCAAGGATA	510	NM_001161371.1	yes
		Rev:	AAACCGCTGCAAACTCCTCA			
SS18L1	CREST	Fwd:	AACCACCGAAGCTCAGCAC	277	NM_178750.5	yes
		Rev:	GGACTCAGCCCGTGATCATT			
RCOR1	Co-REST	Fwd:	CGACTTCGATCCTGCCAAAC	159	NM_198023.2	yes
		Rev:	CCAAGAGCCTGCTCCATGTT			
SMARCC1	BAF155	Fwd:	GCCTTCTTAGAGCAGTGGGG	485	NM_009211.2	yes
		Rev:	AAAGGGACAGGCTGGTAAGC			
ACTL6A	BAF53a	Fwd:	AACACGATGCTGGGAGTCAG	237	NM_019673.2	yes
		Rev:	AGAGCCACCAATCCATGAGC			
ACTL6B	BAF53b	Fwd:	GTCCTACAGCAAGGCATCGT	653	NM_031404.4	yes
		Rev:	CCAATCCAGGGGCTGAACTT			
SMARCD1	BAF60a	Fwd:	CTTATGCCACCAGAGCCCAT	353	NM_031842.2	yes
		Rev:	TAGAACTCAGCACGACGCTC			
PHF10	BAF45a	Fwd:	GTGTCTGAAGGAGGACAGCCC	510	NM_024250.4	yes
		Rev:	GCTGTTTTTCCCCCTTCTGC			
DPF3	BAF45c	Fwd:	ACCTACAAGTGGCAGTGCAT	395	NM_001267625.1	yes
		Rev:	GTCATGGGTAGGGCGAGAAG			
ARID2	BAF200	Fwd:	CAGTATGCAAGAAGCCCCGA	599	NM 175251.4	yes
		Rev:	GCCCAGGTTTTTCTCACTGGA			
SMARCA2	BAF190b	Fwd:	AGCTACGGAGTGGCAAATTC	590	NM_011416.2	yes
		Rev:	TCTCAGCTGCATGATGGTGTT			

Author Manuscript

Author Manuscript

Author Manuscript

Author Manuscript

Hugo nomenclature	Synonyms		Primers (5'-3')	Product size	NCBI Accession number	sequence verified
SMARCA4	BRG1	Fwd:	GAGGGCTACCGCAAACTCAT	942	NM_011417.3	yes
		Rev:	GCGAAGCTGTGGGACAAAAG			
Cyclophilin B	Cyclophilin B	Fwd:	AACAGCAAGTTCCATCGTGT	84	NM 011149.2	
		Rev:	GCTCTTTCCTCCTGTGCCATC			

Table 2

Primers For the mouse pri-miR-9-2 gene locus [*]

Region		Primer sequence	Product Size
pre-mir-9-2	Forward	CCTTGTGAGGGAAGCGAGTT	
coding exon	Reverse	CGTTCCTCGGTGACCTTGAA	112
	Forward	ATTTCCCAAACCCCTCTAGATCC	
1	Reverse	TGGAGACATGCATGATAATGGGA	60
	Forward	CTTCACTCTGCACTCCGAGG	
2	Reverse	GGGAGAGAAAAGGGCGCTAA	101
	Forward	ACATACTGGGGGTCGTCGAA	
3	Reverse	GGCTGTAGTTGTAGCCTGCG	86
	Forward	TGACCTCGCAGCTAAACCTT	
4	Reverse	ACATGCTTTCGGGCTCCAC	81
	Forward	AGCCACCCAAGTCCAGAGAA	
5	Reverse	AGGGAAACAGCGACACCTAC	98

[*] For primer mapping to the pre-miR-9-2 gene, see Figure 4.